

Spatiotemporal wave-train instabilities in nonlinear Schrödinger equation: revisited

Saliya Coulibaly^{1,a}, Eric Louvergneaux¹, Majid Taki¹, and Léo Brevdo²

¹ Laboratoire de Physique des Lasers, Atomes et Molécules, CNRS UMR 8523, Université de Lille Sciences et Technologies, 59655 Villeneuve d'Ascq Cedex, France

² ICube, CNRS UMR 7357, Université de Strasbourg, 2 rue Boussingault, 67000 Strasbourg, France

Received 3 April 2015 / Received in final form 10 June 2015

Published online 28 July 2015 – © EDP Sciences, Società Italiana di Fisica, Springer-Verlag 2015

Abstract. A complete description of properties of the wave-train bifurcating from unstable basic oscillatory states (CW nonlinear stationary states) of the nonlinear Schrödinger equation are studied in the moving frames of reference as an initial value problem and using the methods of absolute and convective instabilities. The predictions are in excellent agreement with numerical solutions and may contribute understanding the nonlinear Schrödinger equation complex dynamics under various initial conditions including, localized and/or noisy initial conditions.

1 Introduction

Since the early work of Rayleigh in the 19th century, for studying linear stability of extended dynamical systems the normal-mode approach – classical linear stability analysis (CLSA) – is traditionally used, see e.g. [1,2]. In this approach, base solutions of the linearized equations of motion having the form of a *monochromatic* wave, $f e^{i(kx - \omega t)}$, are treated, where x is the spatial coordinate, t is the time, k is a wavenumber, ω is a frequency and f is the amplitude of the wave. The base state is unstable when, for some real k , frequency ω has a positive imaginary part. The normal-mode analysis is an indispensable part of any linear stability analysis. However, within the normal-mode approach the dynamics of realistic spatially localized perturbations cannot be treated. In order to address this dynamics one has to treat an initial-value problem formulation for the linearized equations of motion under the assumption of spatially localized initial conditions and, if any, spatially localized boundary conditions.

The theory of evolution of localized disturbances bifurcating from unstable basic state, that is of wave-train, in open systems also known as the theory of absolute and convective instabilities has been developing since the early 1950s, see [3,4]. For two-dimensional homogeneous flows and media, this theory received its sound modern form in reference [5], see also [6] and references therein, and for optics see [7].

A growing wave-train in an open medium can develop according to two essentially different scenarios. In the first scenario, the localized disturbance moves away from the place of its origin, but spreads in space fast enough so that,

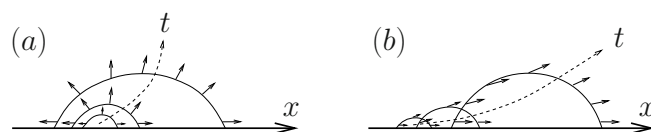


Fig. 1. (a) Absolute instability; (b) convective instability.

at every point of the medium, growth occurs destroying eventually the base state throughout. This is the scenario of absolute instability. In the alternative scenario, the temporally growing wave-train propagates in space more rapidly than it spreads leaving behind, during such a development, a decaying disturbance at every fixed point in space. In this case the medium is called absolutely stable, but convectively unstable. A schematic one-dimensional illustration of the spatiotemporal evolution of the envelope of wave-train in the absolutely unstable case and in the convectively unstable, but absolutely stable case is presented in Figure 1.

The analysis of absolute and convective instabilities provides an important information that cannot be obtained by treating normal modes. It allows one to compute the group velocity of realistic localized disturbances and also to estimate the spatial amplification of such disturbances in the absolutely stable, but convectively unstable case [8,9]. In the latter case one can estimate a portion of the domain in which the state can be viewed as representing a physical end state depending on the spatiotemporal evolution characteristics of the convectively unstable wave-train in the base state, whereas an unstable normal mode is unstable in the entire medium domain.

The theory of absolute and convective instabilities was extended to two-dimensional stationary spatially periodic

^a e-mail: saliya.coulibaly@univ-lille1.fr

media and to the two-dimensional spatially homogeneous temporally oscillating case in references [10,11], respectively. The theory developed in reference [11] was applied in that paper to analyzing the unstable temporally oscillating solutions of the nonlinear Schrödinger (NLS) equation and it was shown that all such solutions are absolutely unstable. Here we apply the above theory to studying the stability characteristics across the wave-train and, in particular, the dependence of the spatio-temporal structure of the wave-train on the observer velocity.

The nonlinear Schrödinger (NLS) equation

$$i\psi_t - s\psi_{xx} + \mathcal{V}'(|\psi|^2)\psi = 0, \quad (1)$$

is used for modeling the dynamics of dispersive waves in a wide variety of nonlinear dynamical systems e.g. in nonlinear optics [12], quantum optics and hydrodynamics (cf. [13] and references therein). In (1), ψ is complex valued, x is a homogeneous coordinate, t is time, and s is 1 (−1) for either defocusing diffractive media or normal dispersion in dispersive ones (for focusing diffractive media or anomalous dispersion in dispersive ones). $\mathcal{V}(\cdot)$ is a real-valued smooth given function.

The sensitivity to the initial condition of systems described by this NLS equation has been widely pointed out during the last years [14]. The phenomenon of sensitivity to noisy (or not) initial condition is not specific to NLS equation but rather an important consequence of convective instabilities giving rise to noise-sustained structures in a wide class of nonlinear systems including hydrodynamic [15] and nonlinear optics [16,17]. Recently many of the aforementioned systems governed by the NLS equation have been shown to exhibit waves with very large amplitude, combined with a particular *L-shape* probability density [18–22]. These solutions have been shown to be strongly nonlinear, giving rise to the appearance of rogue waves that are nowadays widely observed in many systems of nonlinear science [20,23,24]. However, in many cases, the first stage preceding their emergence was shown to be governed by the modulational instability process by means of a classical normal-mode approach. The aim of this study is to respond to the important questions: (i) How a localized initial condition may impact the first stage of the evolution of the nonlinear solutions? (ii) What are their main characteristics during this evolution? For this purpose, we extend the analysis of the NLS equation in reference [11] to studying the characteristics of the unstable linear wave-trains in the moving frames, that is, the properties of the wave-trains such as the temporal amplification rate, the oscillatory frequency, the local wave nature and the local spatial amplification rate across the wave-train solutions.

The paper is organized as follows. In Section 2 we present a concise discussion of the oscillatory solutions of the NLS equation and of stability of such solutions, and also give the general form of the solution of an initial-value problem for localized perturbations. Section 3 describes the treatment of the characteristics of the wave-train as functions of the observer velocity. The spatiotemporal evolution of wave-train is investigated and compared to nu-

merical solutions of NLS equation in Section 4. We discuss our results and conclude in the last Section.

2 Basic oscillatory states of the NLS equation and stability

Equation (1) possesses a family of exact oscillatory solutions

$$\psi_0 = A \exp(i\Omega t) \quad \text{where} \quad \Omega = \mathcal{V}'(|A|^2), \quad (2)$$

with A being complex amplitude.

The basic linear stability properties of the solutions (2) are well established [12]. The destabilization of the solutions plays an important role in the formation of pulse trains, the generation of supercontinuum [25], the subsequent formation of rogue waves [14], and the filamentation process [26]. The linear stability analysis of the basic state ψ_0 under perturbations of the form $\varphi(x, t) \exp(i\Omega t)$ leads to the equation:

$$i\varphi_t - s\varphi_{xx} + \mathcal{V}''(|A|^2) \left(|A|^2 \varphi + A^2 \varphi^* \right) = 0. \quad (3)$$

Within the normal-mode approach, [1], the perturbation is assumed to have the form of a *monochromatic* wave, that is, $\varphi \sim \exp[i(kx - \omega t)]$, where k is a wavenumber and ω is a frequency. We substitute an expression of this form for φ into equation (3) and assuming that $\varphi \neq 0$ obtain that a non-zero monochromatic wave solution exists only for the pairs (k, ω) that satisfy the dispersion relation:

$$D(k, \omega) \equiv \omega^2 - k^4 - 2sk^2 |A|^2 \mathcal{V}''(|A|^2) = 0. \quad (4)$$

The base state is linearly unstable if and only if there exists a real-valued k for which the imaginary part of the corresponding frequency, $\omega = \omega(k)$, is positive. From equation (4) one readily obtains

$$\omega_{1,2}(k) = \pm k \sqrt{k^2 + 2s |A|^2 \mathcal{V}''(|A|^2)}. \quad (5)$$

Hence, for instability it is necessary and sufficient that there exists a real-valued k satisfying $k^2 + 2s |A|^2 \mathcal{V}''(|A|^2) < 0$. Since the parameter s is either 1 or −1, we obtain that the above instability condition holds only for $s = -1$. In what follows only the case $s = -1$ will be considered. Before going further in our study, we note that the above informations (a single wavenumber of the destabilizing mode k (real) and its accompanying complex frequency $\omega_{1,2}(k)$) are all what can be provided by the CLSA. By contrast, in order to determine the linear response of the system to a localized perturbation, it is necessary to include a finite band of modes in the dynamical description. This can be achieved by reformulating the linear stability analysis as an initial-value problem. This makes it possible to determine the main dynamical characteristics of the wave-train bifurcating from the unstable base state including growth rate, instantaneous frequency

and wavenumber and more importantly, its velocity. As it will be shown in the following, the velocity drastically affects the global spatiotemporal growth rate and the spatiotemporal description of the wave-train.

3 Mathematical formalism of absolute and convective instabilities: an initial-value problem

For studying the dynamics of localized linear disturbances, i.e., absolute and convective instabilities, of the base solutions of an extended flow one has to treat a corresponding linear initial-value problem. A treatment of such a problem by using a combined Fourier-Laplace transform and a consistent mathematical formalism for analyzing the asymptotic of the solutions of the problem in the two-dimensional homogeneous case were developed by Briggs [5], see also [6]. Here, we present the form of the solution and sketch the technique for the evaluation of its asymptotic in time in the absolute frame of reference as well as in the moving frames.

In the absolute frame of reference which is the frame of a stationary observer, that is x_0 is fixed, the solution can be expressed as an inverse Fourier-Laplace integral:

$$\varphi(x, t) = \int_{-\infty}^{\infty} dk \int_{i\sigma-\infty}^{i\sigma+\infty} \frac{S(\omega, k)}{D(\omega, k)} e^{i(kx_0 - \omega t)} d\omega, \quad (6)$$

where the function $S(\omega, k)$ represents the external perturbations and, therefore, can be viewed as arbitrary in a certain sense, and $D(\omega, k)$ is the dispersion-relation function (Eq. (4)). In the inverse Laplace integral in (6) the integration is performed along the Bromwich contour [1],

$$\mathcal{B} = \{\omega | \omega_i = \sigma, -\infty < \omega_r < \infty\}, \quad (7)$$

where σ is greater than the maximum growth rate of the monochromatic waves, $\sigma > \sigma_m = \max\{\omega_i | D(k, \omega) = 0, -\infty < k < \infty\}$.

We are also interested in the asymptotic properties of the solution in a frame of reference moving with the velocity V with respect to the absolute frame, that is $x = x_0 + Vt$, where x_0 is fixed. In the moving frame, by a change of variables in the double integral the solution can be brought to the form

$$\varphi(x_0 + Vt, t) = \int_{-\infty}^{\infty} dk \int_{i\sigma-\infty}^{i\sigma+\infty} \frac{S(\omega + Vk, k)}{D(\omega + Vk, k)} \times e^{i(kx_0 - \omega t)} d\omega. \quad (8)$$

Since the function $S(\omega, k)$ representing the external disturbances is in some sense arbitrary, it does not affect the asymptotic properties of the solution. The integral in (8) has a form similar to that of the integral in (6), with $D(\omega + Vk, k)$ being the dispersion-relation function in the moving frame. Hence, the evaluation of the asymptotic behavior of the integrals in (6) and in (8) is similar. We outline here the evaluation procedure for the integral in (6).

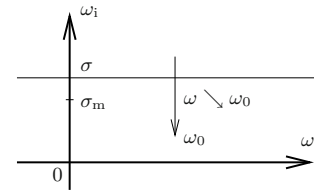


Fig. 2. Movement $\omega \searrow \omega_0$ of ω .

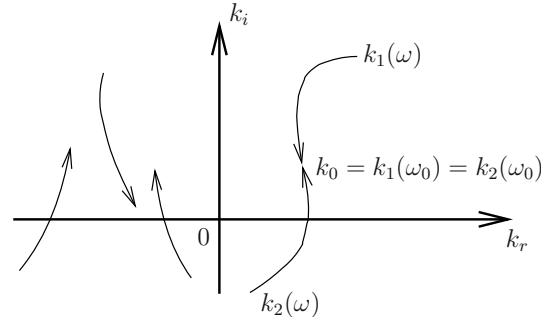


Fig. 3. Collision of two k -roots originating on opposite sides of the real k -axis when $\omega \searrow \omega_0$.

For the evaluation, the Briggs [5] collision criterion (see also [6]) is applied. The collision criterion allows one to identify the points in the upper complex half-plane, $\{\omega_i > 0\}$, that contribute to the growth in time of the solution. For the solution given in (6) the identification is performed as follows. Let ω_0 be a point in the upper complex half-plane and let $\omega \searrow \omega_0$ denote a movement of the point ω along the vertical line passing through ω_0 from above the Bromwich contour till ω_0 , as illustrated in Figure 2. Let $k_n(\omega), n = 1, 2, \dots$, be all the k -roots of $D(k, \omega) = 0$. For ω laying above the Bromwich contour, all the k -roots are located away from the real k -axis because $\sigma > \sigma_m$. When $\omega \searrow \omega_0$ the k -roots move in the complex k -plane. The point ω_0 contributes to the growth of the solution if and only if, in the most common case, two of the k -roots originating on opposite sides of the real k -axis collide when ω reaches the point ω_0 in the movement $\omega \searrow \omega_0$. This type of a collision is called a pinching collision. Generally, a collision of several k -roots with, at least, two roots originating on opposite sides of the real k -axis produces a point ω_0 contributing to the instability [7,27]. However, commonly only collisions of two roots are present. One such a collision is illustrated in Figure 3.

At the collision point, $k = k_0$, the function $D(k, \omega)$ has a double root in k and, hence, at $(k, \omega) = (k_0, \omega_0)$ it holds that

$$D(\omega, k) = 0, \quad \frac{\partial D(\omega, k)}{\partial k} = 0. \quad (9)$$

A branch of the function $\omega = \omega(k)$ has at the collision point a simple stationary point satisfying $\frac{d\omega(k_0)}{dk} = 0$. A contribution to the asymptotic of the solution, $\varphi(x, t)$, as $t \rightarrow \infty$, from a point $\omega = \omega_0$ satisfying the collision criterion is given by:

$$C(x_0, \omega_0) = a(k_0, \omega_0, x_0) \frac{1}{\sqrt{t}} e^{ik_0 x_0} e^{-i\omega_0 t}, \quad (10)$$

where $k = k_0$ is the collision point as described above. In the cases when the k -roots of $D(k, \omega) = 0$, cannot be analytically explicitly computed but can rather be numerically calculated, the points satisfying the collision criterion can be found by following the movement of the images of the Bromwich contour on the complex k -plane under the transformations $k = k_n(\omega)$, $n = 1, 2, \dots$, and identifying the collision points of the images originating on opposite sides of the real k -axis, as ω varies from above $\omega_i = \sigma_m$ down to zero [7,27]. The asymptotic of the solution in time along a ray $x = x_0 + Vt$, with $V \neq 0$, that is, the asymptotic of the integral in (8) is evaluated similarly.

An evaluation of the asymptotic of the solution can in principle also be performed by finding all the saddle points in the upper ω -half-plane of all the branches of the function $\omega = \omega(k)$ and applying the steepest descent method at every such a point. However, the crucial task in such a procedure is to prove the existence of the global steepest descent contour which is equivalent to the real k -axis. As a matter of fact, the mere existence of a saddle point in the upper ω -half-plane does not guarantee at all that the point contributes to the growing asymptotic of the solution, see a discussion in reference [28]. In particular, it has been shown in reference [27] that in the Eady model of a geophysical flow [29], there exists an infinite number of saddle points in the upper ω -half-plane none of which contributes to the growing asymptotic of the solution.

4 Description of wave-train bifurcating from the base state of the NLS equation

The formalism of absolute and convective instabilities for two-dimensional homogeneous flows developed in reference [5] was extended to spatially periodic flows and, respectively, to temporally oscillating flows by Brevdo and Bridges [10,11], respectively. In the temporally oscillating case which is of interest in the present study, an initial-value problem formulated for an equation with time-periodic coefficients is treated by a Fourier transform, then by a Floquet transform and finally by a Laplace transform. The solution of the initial-value problem is expressed as an inverse Fourier-Laplace integral of a form similar to that of the integral in (6). As a consequence, the method for studying the dynamics of wave-train described in the previous section applies in this case.

In reference [11], the asymptotic of the unstable wave-train of the NLS equation in the *absolute frame* of reference were studied and it was shown that all the oscillatory base solutions of the NLS equation are *absolutely unstable*. The asymptotic profile of the wave-train of the NLS equation in the moving frames were treated in reference [30] by using the steepest descent method in the framework of the saddle-point approach. In the present paper, we extend the consistent theory in reference [11] to moving frames in order to identify absolutely stable but convectively unstable domains. More importantly, we apply the collision criterion for analyzing the structure of wave-train of the NLS equation and obtain the results which are in good agreement with the results obtained in reference [30].

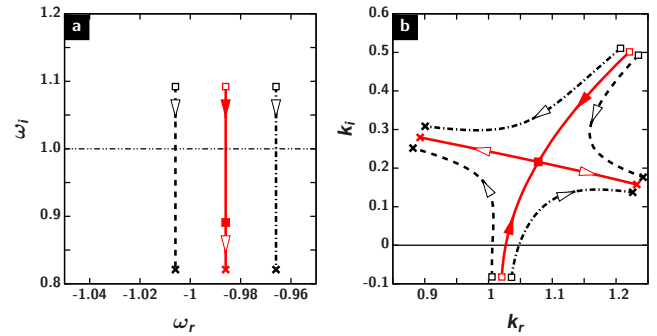


Fig. 4. Illustration of the pinching collision for $b = 1$ and $V = 0.96$.

In the latter, the crucial question in a saddle-point treatment of the existence of a global steepest descent contour for the saddle point which lies entirely in the valley of the ω -branch and is equivalent to the real k -axis was not addressed. However, good agreement between our results and the results in reference [30] implies that in this particular case the saddle-point approach works.

In the case under consideration, the solutions of the system corresponding to system (9) for a frame moving with velocity V with respect to the absolute frame,

$$D(\omega + Vk, k) = 0, \quad \frac{\partial D(\omega + Vk, k)}{\partial k} = 0, \quad (11)$$

can explicitly be calculated. The solutions are given by:

$$k_{1,2,3,4}^0 = \pm \sqrt{b + \frac{V^2}{8} \pm \frac{V}{2} \sqrt{\frac{V^2}{16} - b}}, \quad (12)$$

where $b = |A|^2 \mathcal{V}''(|A|^2)$. By using these notations, the corresponding values of ω are expressed as:

$$\omega_{1,2}(k) = -kV \pm k\sqrt{k^2 - 2b}. \quad (13)$$

The maximum growth of the normal modes, $\sigma_m = b$, is attained at $k = \pm\sqrt{b}$. From (12) one can see that for $|V| < 4\sqrt{b}$ all the k^0 -roots are complex-valued and it holds that $k_1^0 = -k_2^0 = k_3^{0*} = -k_4^{0*}$, where the asterisk denotes the complex conjugate. When $|V| \geq 4\sqrt{b}$ all the k^0 -roots are real-valued, with $k_1^0 = -k_2^0$ and $k_3^0 = -k_4^0$.

In Figure 4, the movement $\omega \searrow \omega_0$ and a collision of two k -roots of $D(\omega + Vk, k) = 0$ originating on opposite sides of the real k -axis are shown by solid curves for the case $b = 1$ and $V = 0.96$. In this case $\omega_0 = -0.98593 + 0.890795i$ and $(k_r^0, k_i^0) = (1.07791, 0.216129)$. To illustrate the mapping of ω to the complex k -plane close to the point of collision we present in this figure also the movements $\omega \searrow \omega_0 \pm \epsilon$, with $\epsilon = 0.02$ and the trajectories of the corresponding k -roots in the k -plane by using dotted $(\omega_0 - \epsilon)$, and dotted-dashed $\omega_0 + \epsilon$, curves, respectively.

Then, repeating the aforementioned procedure we have obtained the following results (see Fig. 5):

- (i) k_1^0 : in the region $0 \leq V \leq 4\sqrt{b}$, this branch can be written in the form $k_1^0 = ks(V) = ks_r(V) + iks_i(V)$

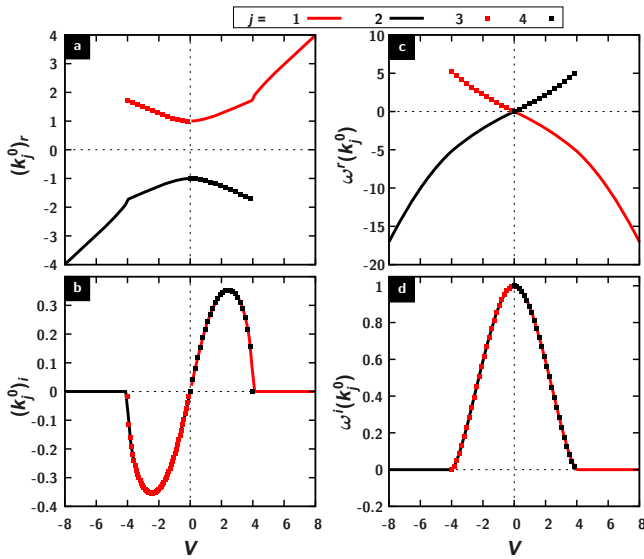


Fig. 5. Evolution of the real (a) and imaginary (b) parts of the contributing saddle points. The real and imaginary part of the corresponding ω branches are given by (c) and (d), respectively.

with $ks_r \geq 1$ and $ks_i > 0$. When collisions occur on this branch, $\text{Re}(\omega) < 0$ which correspond to ω_1 branch in Fig. 5c). For $V \geq 4\sqrt{b}$, $k_1^0 = ks_r > 0$ is purely real and the collisions are observed also for $\text{Re}(\omega) < 0$ but with $\text{Im}(\omega) = 0$.

- (ii) k_2^0 : in the region $-4\sqrt{b} \leq V \leq 0$, this branch can be written in the form $k_2^0 = -ks_r(V) - iks_i(V)$. When collisions occur on this branch, $\text{Re}(\omega) < 0$ which correspond to ω_2 branch. For $V \leq -4\sqrt{b}$, $k_2^0 = -ks_r$ is purely real and the collisions are observed also for $\text{Re}(\omega) < 0$ but with $\text{Im}(\omega) = 0$.
- (iii) k_3^0 : in the region $-4\sqrt{b} \leq V \leq 0$, we have $k_3^0 = ks_r(V) - iks_i(V)$. When collisions occur on this branch, $\text{Re}(\omega) > 0$ which correspond to ω_2 branch.
- (iv) k_4^0 : in the region $0 \leq V \leq 4\sqrt{b}$, we have $k_4^0 = -ks_r(V) + iks_i(V)$. When collisions occur on this branch, $\text{Re}(\omega) > 0$ which correspond to ω_1 branch.

That is, complex type contributing points ($-4\sqrt{b} \leq V \leq 4\sqrt{b}$) correspond to locally growing solutions. In addition, in this region we observe a degeneracy of the imaginary part of the contributing points which leads to the degeneracy of the growing rate $\text{Im}(\omega)$. In contrast, purely real contributing points ($V \leq -4\sqrt{b}$ and $V \geq 4\sqrt{b}$) are marginal solutions and no degeneracy is observed. Based on these results, in the region of complex type contributing points, we find the following relations between the contributing part in the integrands:

$$\begin{aligned} \omega_1(k_1^0, V > 0) &= \omega_2(k_2^0, V < 0) = S(ks, V), \\ \omega_1(k_4^0, V > 0) &= \omega_2(k_3^0, V < 0) = S^*(ks, V), \end{aligned}$$

with

$$S(ks, V) = -ks|V| + ks\sqrt{ks^2 - b}. \quad (14)$$

After lengthy but straightforward calculations we obtain, from (8), the asymptotic shape of the impulse response as:

$$\varphi(Vt, t) \simeq \begin{cases} \sqrt{\frac{1}{2\pi t}} \left[\text{Re} \left(\sqrt{\frac{1}{iS''}} \exp(iSt) \right) + i \text{Im} \left(\sqrt{\frac{1}{iS''}} \alpha(ks) \exp(iSt) \right) \right] & \text{if } |V| \leq 4\sqrt{b}, \\ \sqrt{\frac{1}{2\pi t}} \left[1 + \frac{\sqrt{ks_0^2 - 2}}{ks_0} \right] \sqrt{\frac{1}{iS''}} \exp(iSt) & \text{if } |V| \geq 4\sqrt{b}, \end{cases} \quad (15)$$

where $\alpha(k) = \sqrt{k^2 - 2b}/k$ and the primes correspond to the derivative with respect to k . This result was also obtained in a previous work [30], but without checking the pinching condition. In Figure 6 we have plotted this profile after a propagation distance $t = 30$ together with the result of the numerical integration of equation (1). As can be seen from this figure we have an excellent agreement between the two results. It is worthy to stress some intriguing differences between the results presented here and the standard modulational instability that appears in this system. The first point that we would emphasize is the existence of a band of modulational instability in which no saddle point can be found. Indeed, as can be seen from Figure 5a the region $-1 \leq \text{Re}(k^0) \leq 1$ is free of any saddle point while the standard analysis predicts the whole band $-\sqrt{2} \leq \text{Re}(k) \leq \sqrt{2}$ to be unstable. In addition we have obtained here that the unstable band is locally extended up to $|\text{Re}(k^0)| = \sqrt{3}$. Since the Fourier spectrum fails to capture these properties of the wave-train we need an appropriate method that allows the access to the local phase. For this end, we have computed the Hilbert transform of the impulse response. However, it is well-known that the accuracy of the instantaneous frequency obtained from the numerical Hilbert transform is relevant close to the dominant component of the Fourier spectrum that is, around the center of the pulse. In order to improve the detection of the local wavenumber we have computed the wavelet transform of the signal and then calculated the ridges of this transform, which produces the (+) symbols in Figure 7, showing an excellent agreement with the analytical predictions.

5 Discussion and concluding remarks

The evolution of a growing disturbance in both space and time is drastically different from those obtained by the CLSA (normal mode theory). The initial value problem formulation shows the key role played by the observer velocity (group velocity) in the modulational instability process. Indeed, despite the appearance of a band gap in the frequencies excited locally, we observe an extension of the instability region outside the standard modulational instability limit. This also suggests that the instability gain seen by an observer is closely related to the velocity with which this one is moving. In order to verify this statement we track the position of a given local frequency along the

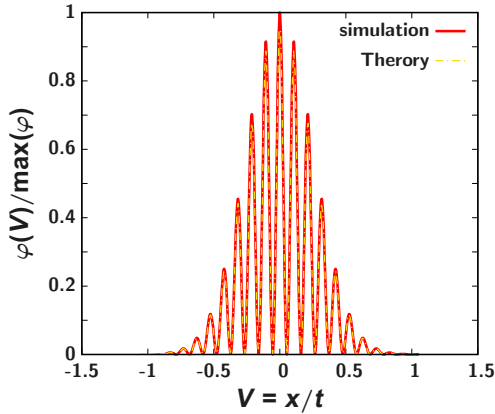


Fig. 6. Profile of the impulse response obtained from equation (15) (solid line) and from numerical integration of equation (1) (dot-dashed line).

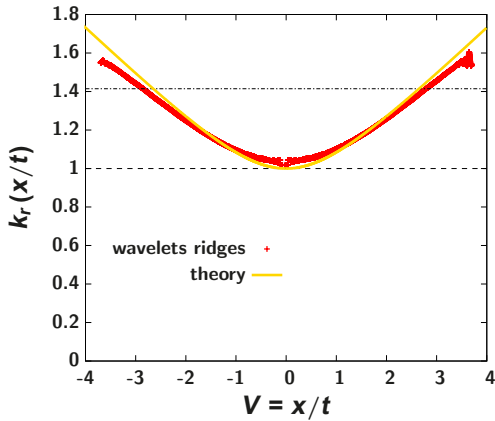


Fig. 7. Local wavenumber of the impulse response (solid line) and the wavelet ridges (+) of the numerical result of Figure 6.

propagation which allows us to compute the associated velocity. Next, considering this velocity we compute the corresponding global gain. Repeating this process leads to the mapping of the global gain with respect to the velocity and implicitly with respect to the local wavenumber as can be seen in Figure 8. This map of the global gain with respect to the local wavenumber can be obtained theoretically by making a parametric plot from the analytical expression (solid lines in Fig. 8), which shows a good agreement between the two results. Note that since the global gain is symmetric in k , we only show in Figure 8 the analytical results for $k > 0$. A question now arises as what happens if an observer moves with a velocity outside the range $-4 \leq V \leq 4$ (see Fig. 5)? In that case, according to equation (15) this observer will see a wave-train experiencing an attenuation ruled by a $t^{-1/2}$ power law since S is real and the exponential term is oscillating ($\text{Im}(\omega) = 0$). This behavior constitutes another fundamental difference between the initial value problem approach and that of normal mode. Indeed, in the later approach a plane wave with a wavenumber outside the instability band will be neither amplified nor attenuated (marginally stable mode), meanwhile in the initial value

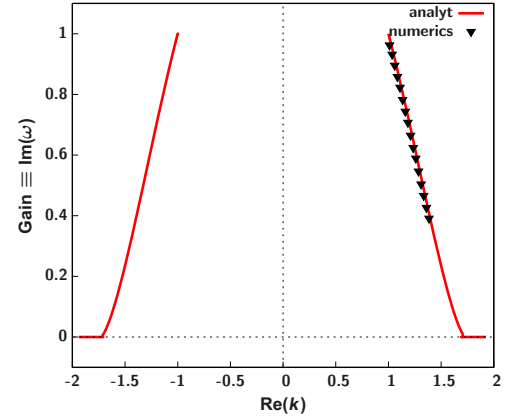


Fig. 8. Analytical (solid line) and numerical (triangles) local gain curves of an impulse perturbation.

problem formulation no marginal situation can exist. This behavior is illustrated in Figure 9, where we have plotted the inverse of the intensity across the time with two velocities $V = 5$ and $V = 12$ which gives a linear evolution as predicted by the above power law.

Let us now concentrate on the fact that no local wavenumber exists in the band $|k_r^0| < 1$ (see Fig. 5a). It is understandable that this result means that starting with a narrow band localized state, the spontaneous solution that will form will be that given by equation (15). However, the question may arise about the wave number k_r^0 such that $|k_r^0| < 1$. To elucidate this question we can benefit from the asymptotic solution previously derived. Indeed, this expression is an estimation of the Green function, i.e., the linear impulse response of the system. That is, as well as we have computed the instantaneous wave numbers of this solution, we can also compute the *group displacement*. Hence, in addition to have an access to the mean position of the pulse, this curve can provide an insight about whether an initial pulse centered around a given wavenumber will experience some distortions effects. By analogy to the *group delay* of a temporal pulse, here, the *group displacement* is used to quantify the variation of the translational shift as a function of the wavenumber of an impulse traveling through the system. Further and deep discussion about the *group delay* concept can be found in reference [31].

The estimation of the *group displacement* from both analytical and numerical pulse have been carried out. However, since the two results are almost mingled we only show here that obtained from the numerical solution in Figure 10. As can be seen from this figure, the *group displacement* is zero for $0.6 \leq k \leq 1.7$ and presents fast variations elsewhere. On the other hand it appears from this result that starting with a pulse with central wavenumber lying in the aforementioned region will not produce any distortion, whereas any initial pulse with central wavenumber outside this region will experience some distortions leading to a non-localized structure as can be seen in Figure 11. Indeed, in this figure we have plotted the output signal that emerges from an initial Gaussian

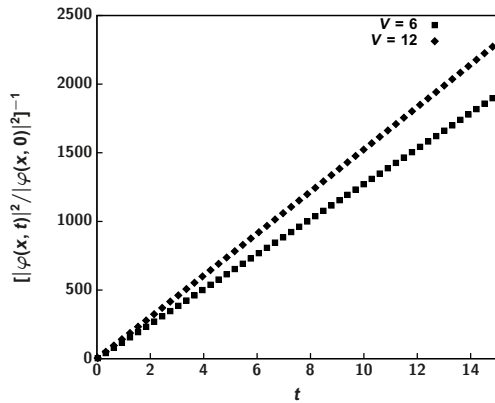


Fig. 9. Evolution of the inverse of the normalized intensity for an observer moving with $V = 6$ (squares) and $V = 12$ (diamonds).

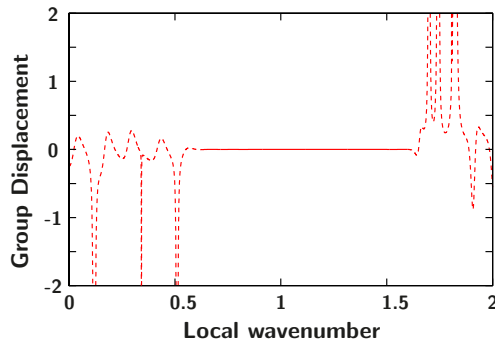


Fig. 10. Group Displacement of the linear impulse response of equation (1).

pulse at $k = 0.3, 1.2$ and 1.8 . As expected from the above *group displacement*, the pulses at 0.3 and 1.8 experience distortion effects while the pulse at 1.2 is free from any distortion effects.

In conclusion, we have estimated by means of an initial-value problem formalism, the linear impulse response associated with continuous wave (cw) solutions of the Nonlinear Schrödinger equation. This approach allows us to compute the global (spatiotemporal) gain of the system which displays a gap in the band of standard modulationally unstable wavenumbers. We also show through the determination of the *group displacement* that this band gap induced a region of wavenumbers where the *group delay* vanishes. In this region we have observed that pulses maintain their shape without distortion. However, any initial pulse with a wavenumber outside this region evolves to a distorted output pulse. Finally, owing to the ubiquitous nature of the NLS equation in nonlinear science, the results obtained here can be applied to such diverse fields as the hydrodynamics, plasma physics, and nonlinear optics.

This research was supported by the Interuniversity Attraction Poles program of the Belgian Science Policy Office under the grant IAPP7-35, the French Project ANR Blanc OptiRoc N12-BS04-0011, and the “Laboratoire d’Excellence: Centre

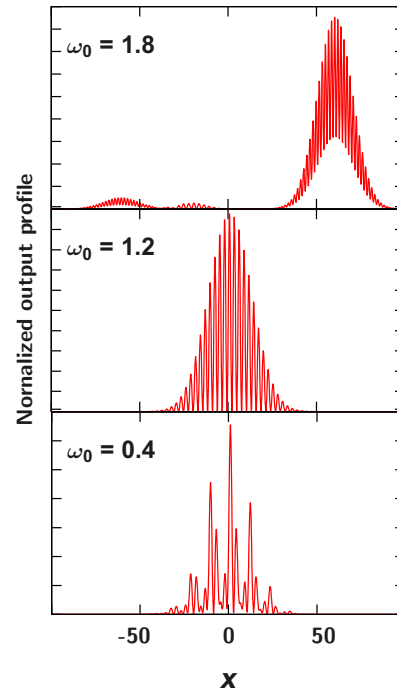


Fig. 11. Normalized output profiles corresponding to Gaussian initial perturbations ($\varphi(x, 0) \propto e^{-(x/20)^2} e^{-ik_0 x}$). Integration time is $t = 30$.

Européen pour les Mathématiques, la Physique et leurs Interactions” CEMPI.

References

1. P.G. Drazin, W.H. Reid, *Hydrodynamic stability* (Cambridge University Press, 2004)
2. S. Chandrasekhar, *Hydrodynamic and hydromagnetic stability* (Dover Publications, New York, 1981)
3. L.D. Landau, E.M. Lifshitz, *Electrodynamics of Continuous Media* (GITTL, Moscow, 1953)
4. R.Q. Twiss, Proc. Phys. Soc. Lond. B **64**, 654 (1951)
5. R.J. Briggs, *Electron-stream Interaction with Plasmas* (MIT Press, Cambridge, 1964)
6. A. Bers, in *International Congress on Waves and Instabilities in Plasmas*, edited by G. Auer, F. Cap (Innsbruck, 1973), pp. B1–B52
7. H. Ward, M.N. Ouarzazi, M. Taki, P. Glorieux, Phys. Rev. E **63**, 16604 (2001)
8. L. Brevdo, Z. Angew. Math. Mech. **74**, T340 (1994)
9. S. Coulibaly, M. Taki, N. Akhmediev, Opt. Lett. **36**, 4410 (2011)
10. L. Brevdo, T.J. Bridges, Phil. Trans. Roy. Soc. Lond. A **354**, 1027 (1996)
11. L. Brevdo, T.J. Bridges, Z. Angew. Math. Phys. **48**, 290 (1997)
12. G.P. Agrawal, *Nonlinear Fiber Optics*, 3rd edn. (Academic Press, Boston, 2008)
13. J.T. Stuart, R.C. DiPrima, Proc. Roy. Soc. Lond. A **362**, 27 (1978)
14. M. Taki, A. Mussot, A. Kudlinski, E. Louvergneaux, M. Kolobov, M. Douay, Phys. Lett. A **374**, 691 (2010)

15. K.L. Babcock, G. Ahlers, D.S. Cannell, Phys. Rev. Lett. **67**, 3388 (1991)
16. M. Santagiustina, P. Colet, M. San Miguel, D. Walgraef, Phys. Rev. Lett. **79**, 3633 (1997)
17. E. Louvergneaux, C. Szwaj, G. Agez, P. Glorieux, M. Taki Phys. Rev. Lett. **92**, 043901 (2004)
18. D.R. Solli, C. Ropers, P. Koonath, B. Jalali, Nature **450**, 1054 (2007)
19. M. Erkintalo, G. Genty, J.M. Dudley, Eur. Phys. J. ST **185**, 135 (2010)
20. N. Akhmediev, J.M. Soto-Crespo, A. Ankiewicz, Phys. Lett. A **373**, 2137 (2009)
21. K. Hammani, B. Kibler, C. Finot, A. Picozzi, Phys. Lett. A **374**, 3585 (2010)
22. A. Mussot, A. Kudlinski, M. Kolobov, E. Louvergneaux, M. Douay, M. Taki, Optics Express **17**, 17010 (2009)
23. C. Kharif, E.N. Pelinovskii, A. Slunyaev, *Rogue Waves in the Ocean* (Springer-Verlag, Berlin, 2009), Chap. 4 and references therein
24. M. Onorato, S. Residori, U. Bortolozzo, A. Montina, F.T. Arecchi, Phys. Rep. **528**, 47 (2013)
25. J.M. Dudley, G. Genty, S. Coen, Rev. Mod. Phys. **78**, 1135 (2008)
26. V.I. Bespalov, V.I. Talanov, J. Exp. Theor. Phys. Lett. **3**, 307 (1966)
27. L. Brevdo, Geophys. Astrophys. Fluid Dyn. **40**, 1 (1988)
28. L. Brevdo, P. Laure, F. Dias, T.J. Bidges, J. Fluid Mech. **396**, 37 (1999)
29. J. Pedlosky, *Geophysical Fluid Dynamics* (Springer-Verlag, New York, 1987)
30. M. Yu, C.J. McKinstrie, Phys. Rev. E **52**, 6826 (1995)
31. B. Boashash, Proc. IEEE **80**, 520 (1992)